

Studies of the underlying event in ATLAS

Sebastian Wahrmund*

On behalf of the ATLAS Collaboration

Institut für Kern- und Teilchenphysik an der TU Dresden, 01069 Dresden, Germany

September 11, 2013

Abstract

Particle distributions sensitive to the underlying event have been measured with the ATLAS detector at the LHC at the center-of-mass energy of 7 TeV. Charged particle multiplicity, charged and inclusive sum transverse momentum densities and mean charged-particle transverse momentum in the regions of each event, azimuthally transverse to the hardest jet, are presented. The underlying event properties are investigated for minimum bias events and events with jets. When compared to the predictions of different Monte Carlo models, the data show sensitivity to the modeling of the underlying event.

1 Introduction

The hard scattering process of two protons consists of several sub-reactions at different energy scales, leading to a complex collision landscape. Besides a hard interaction at a high energy scale, which is normally used to trigger the event, the scattering process includes several sub-interactions like: additional parton-parton scattering processes within the same proton-proton collision, termed multiple parton interaction (MPI), interaction of the beam-beam remnants as well as contributions from initial and final state radiation. All these additional interactions are collectively termed the “underlying event” (UE).

This report will give an overview about the underlying event measurements using dijet events. The analysis was performed using proton-proton collisions measured with ATLAS experiment [1] at a center-of-mass energy of 7 TeV and an integrated luminosity of 37 pb^{-1} . More details on the analysis can be found in [2].

Presented at the Low x workshop, May 30 - June 4 2013, Rehovot and Eilat, Israel
*sebastian.wahrmund@tu-dresden.de

2 Analysis

The strategy is to identify regions to help in the separation of the hard interaction process and the underlying event. Therefore the direction and energy flow of the hard process is defined by the transverse momentum, p_T^{lead} , of the jet with the highest transverse momentum within the event. Jets used in this analysis are reconstructed using the anti- k_T algorithm [3] with a resolution parameter of $R = 0.4$. Input for the jet algorithm are so-called topological cluster of energy deposits in the ATLAS calorimeter cells [4]. The definition of the hard interaction allows a division of the azimuthal space transverse to the beam direction into three regions:

1. Toward: $\Delta\phi < 60^\circ$
2. Transverse: $60^\circ < \Delta\phi < 120^\circ$
3. Away: $120^\circ < \Delta\phi$

in which $\Delta\phi = |\phi_{\text{lead}} - \phi_{\text{track, cluster}}|$ is the angular separation between the leading jet and a corresponding track or topological cluster respectively. The transverse region is sensitive to the underlying event, since it is perpendicular to the hard scattered plane. The toward and away regions are dominated by the activity of the leading jet and the corresponding balancing jet in the away region. In addition it is useful to define the trans-max/trans-min regions which correspond to the transverse region with the highest/lowest activity for a given observable. The full event selection is described in Section 2.1 and the measured observables in Section 2.2.

2.1 Event selection

Two different event topology are studied within this analysis.

Inclusive jet topology This provides the least biased measurement of the underlying event activity and allows a comparison with other underlying event measurements. Events need to be recorded during stable beam conditions and with all necessary detector components fully operational. The events need to be triggered either by minimum bias or jet trigger based on the transverse momentum of the leading jet. The leading jet needs to have a minimal transverse momentum of 20 GeV and a rapidity of $|y_{\text{lead}}| < 2.8$. To ensure a high vertex reconstruction efficiency, the primary vertex is required to have at least 5 associated tracks each with at least a p_T of 400 MeV. Events with more than one vertex, each with at least 2 tracks, are removed in order to reduce the contamination of additional proton-proton scatterings during the bunch crossing.

Exclusive dijet topology The exclusive selection is a dijet selection, which is performed on top of the inclusive jet topology selection. An additional, sub-leading, jet with $p_T^{\text{sub-lead}} > 20$ GeV and $|y_{\text{sub-lead}}| < 2.8$ is required. The

leading and sub-leading jet need to form a back-to-back topology, in order to avoid any additional radiation of the hard interaction in the transverse region. This is enforced by a cut on $|\Delta\phi_{\text{lead,sub-lead}}| > 2.5$ between the leading and sub-leading jet as well as p_T balance requirement, $\frac{p_T^{\text{sub-lead}}}{p_T^{\text{lead}}} > 0.5$. In addition all events including a third jet with $p_T > 20$ GeV are removed. These additional separation steps reduce the contribution of the hard scattering in the transverse region and allows a cleaner measurement of the underlying event activity. However this selection can also bias the underlying event measurement, by vetoing potential events with a third jet coming from MPI.

2.2 Observables

The properties of the underlying event are measured using track and calorimeter cluster based observables within the transverse region. The selected tracks are required to have $p_T > 500$ MeV and $|\eta| < 2.5$. The topological calorimeter cluster are required to be within either $|\eta| < 2.5$ or $|\eta| < 4.8$. Both tracks and cluster need to fulfill certain quality criteria to ensure well reconstructed objects [5, 6].

Track based observables:

$\langle d^2 N_{\text{ch}}/d\eta d\phi \rangle$: Mean number of stable charged particles

$\langle d^2 \sum p_T/d\eta d\phi \rangle$: Mean scalar p_T sum of stable charged particles

$\langle p_T \rangle$: Average p_T of stable charged particles

Cluster based observables:

$\langle d^2 \sum E_T/d\eta d\phi \rangle$: Mean E_T sum of stable charged and neutral particles

3 Correction Procedure

The unfolding to correct for detector effects is necessary in order to compare the measurements directly with various model predictions, without the need of an additional detector simulation. Two correction steps are performed:

The first step is the correction for track reconstruction inefficiency as well as misidentified tracks from secondary interactions. The track reconstruction efficiency, ϵ_{trk} , and the fraction of secondary particles, f_{sec} were studied within minimum bias measurements [5] at ATLAS. Track based observables are corrected by applying the following weight to correct for reconstruction inefficiency:

$$w_{\text{trk}} = \frac{1}{\epsilon_{\text{trk}}}$$

and the following weight to account for secondary particles:

$$w_{\text{sec}} = (1 - f_{\text{sec}}).$$

The effects of fake tracks as well as tracks from particles which migrated into and out of the kinematic range are studied and found to be negligible.

The second correction steps is a Bayesian unfolding procedure described in [7]. It is used to correct the cluster based observables and to remove additional detector effects for the track based observables, which are not covered by the weighting process. Therefore the Bayesian unfolding process is performed on top of the weighting correction factors. The method is based on the following relation between the number of reconstructed events in the bin j , $n(R_j^{\text{data}})$, and the corrected data events in bin i , $n(C_i^{\text{data}})$:

$$n(C_i^{\text{data}}) = \sum_j P(T_i^{\text{MC}}|R_j^{\text{MC}}) n(R_j^{\text{data}})$$

in which $P(T_i^{\text{MC}}|R_j^{\text{MC}})$ is the unfolding matrix. This matrix can be expressed using the Bayesian theorem:

$$P(T_i^{\text{MC}}|R_j^{\text{MC}}) = \frac{P(R_j^{\text{MC}}|T_i^{\text{MC}})P(T_i^{\text{MC}})}{P(R_j^{\text{MC}})}$$

in which $P(R_j^{\text{MC}}|T_i^{\text{MC}})$ describes the probability that a truth event in bin i will migrate in bin j of the reconstructed event. This smearing matrix contains the full information of the detector effects and is calculated using Monte Carlo (MC) detector simulations. $P(T_i^{\text{MC}})$ is the initial prior probability, which is unknown. In order to avoid any dependence on the choice of the prior probability, the process of unfolding is performed iteratively, using the corrected data of one iteration process as the new prior for the next iteration steps. The process of iteration is performed until the corrected data converge to a state, which remains stable with an increasing number of iteration steps.

4 Results

This section will summarize the results. The measured data points are fully corrected back to particle level as described in Section 3 and are compared to Monte Carlo generator prediction, without any additional detector simulation. The following event generators are used for comparison:

- PYTHIA 6 [8] with the AUET2B [9] and DW [10] tune
- Pythia 8 [11] with the AU2 [12] CT10 [13] tune
- HERWIG/JIMMY [14] with ATLAS AUET2 [9] LO** tune
- ALPGEN+HERWIG/JIMMY [15] with AUET1 [9] CTEQ6L1 [16] tune

- Herwig++ [14] with the UE7-2 [17] tune

The distributions for the mean transverse momentum sum and multiplicity of charged particles are presented in Figure 1 as a function of p_T^{lead} . Both observables increase with rising p_T^{lead} for the inclusive topology but they stay constant for the exclusive dijet selection and start to decrease for high values of p_T^{lead} . A similar trend can be observed for the trans-max region but not for trans-min, as can be seen in Figure 2, which is constant against p_T^{lead} with a slight decrease for high p_T^{lead} values in the exclusive case. These features give an indication that the underlying event is nearly independent of the hard scattering scale, since the trans-min region and the full exclusive topology are constructed to contain as less contamination of the hard scattering as possible. The decrease in the exclusive topology for high p_T^{lead} values can give an indication for a potential bias of the underlying event, by vetoing events with jets produced in underlying event reactions. The same behavior can be observed for the mean transverse energy sum of charged and neutral particles in Figure 3. All MC generators are able to reproduce the basic features of the distributions to a certain amount but show differences in the overall normalization compared to the measurement. The mean p_T of the of charged particles is presented in Figure 4. The distributions against p_T^{lead} show an increasing behavior for increasing values of p_T^{lead} in the inclusive topology but remains constant in the exclusive case. The mean p_T against charge particle multiplicity instead is slightly rising for an increasing number of charged particle in the inclusive as well as the exclusive topology. In both case the main shapes of the distributions are reproduced by MC models within an uncertainty of 10-20%.

5 Summary

The underlying event analysis in inclusive jet and exclusive dijet events is performed up to a leading jet energy scale of 800 GeV. An increasing level of activity against p_T^{lead} is seen for the inclusive topology except for the trans-min region but a constant level activity is observed for the exclusive topology. In this case the selection removes additional contributions of the hard scattering in the transverse plane and allows a cleaner measurement of the underlying event activity. For higher values of p_T^{lead} , a decrease of the UE activity was observed in the exclusive region, which indicates a potential bias, by removing event with additional jet above 20 GeV origination from underlying event interactions. In the most cases the MC models are able to reproduce the underlying event distributions within the 10-20 % measurement uncertainty.

References

- [1] ATLAS Collaboration JINST **3** (2008) S08003.
- [2] ATLAS Collaboration Dec, 2012.
<https://cds.cern.ch/record/1497185>. ATLAS-CONF-2012-164.

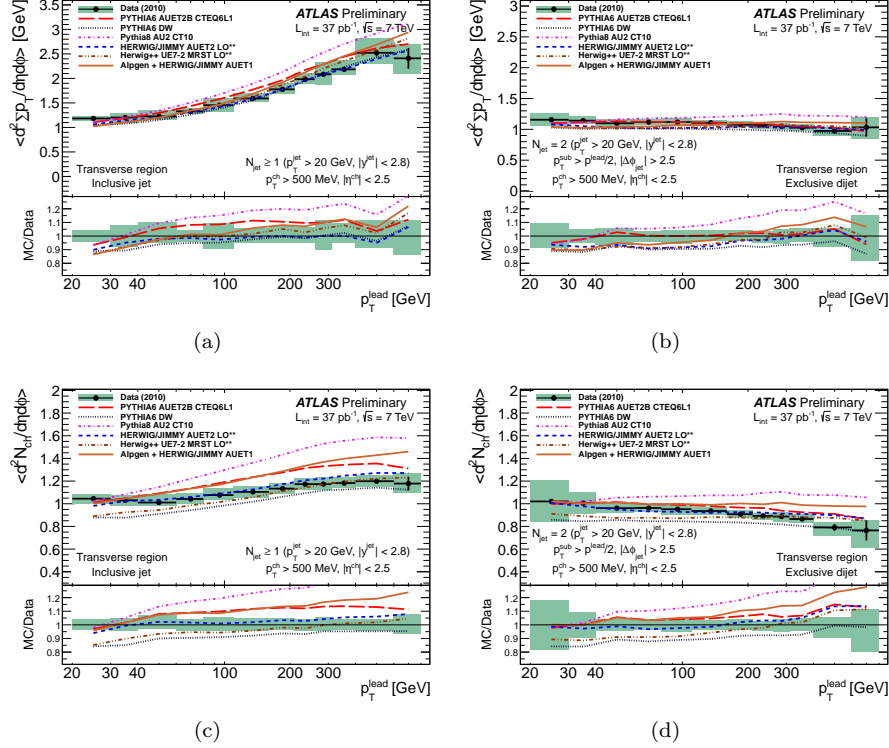


Figure 1: Profile distributions for the transverse momentum sum of charged particles (top) and the multiplicity of charged particle (bottom) are presented for the inclusive jet (left) and exclusive dijet topology (right). The results are shown for the full transverse region and compared to several Monte Carlo event generator predictions. The black error bar indicate the statistical uncertainty on the data measurements and the green shaded area the combined statistical and systematic uncertainty. Results are taken from [2].

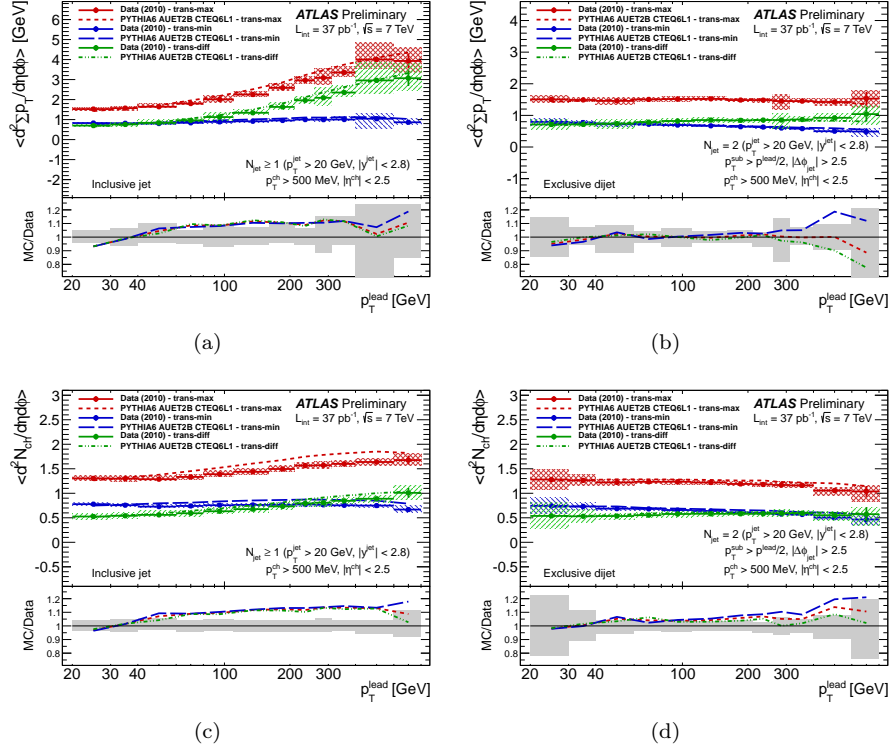


Figure 2: Profile distributions for the transverse momentum sum of charged particles (top) and the multiplicity of charged particle (bottom) are presented for the inclusive jet (left) and exclusive dijet topology (right) and the trans-max, trans-min and trans-diff region, which shows the difference between max and min. The results are compared to PYTHIA6 AUET2B predictions. The error bars indicate the statistical uncertainty on the data measurements and the shaded areas the combined statistical and systematic uncertainty. Results are taken from [2].

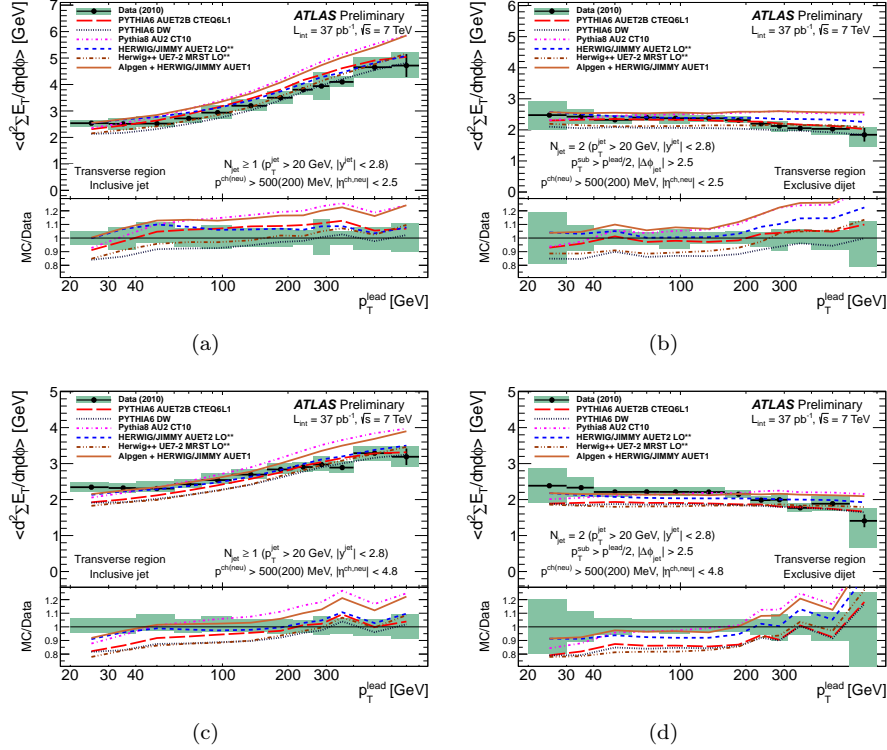


Figure 3: Profile distributions for the transverse energy sum of charged and neutral particles in the central region (top) and for the full detector (bottom) are presented for the inclusive jet (left) and exclusive dijet topology (right). The results are shown for the full transverse region and compared to several Monte Carlo event generator predictions. The black error bar indicate the statistical uncertainty on the data measurements and the green shaded area the combined statistical and systematic uncertainty. Results are taken from [2].

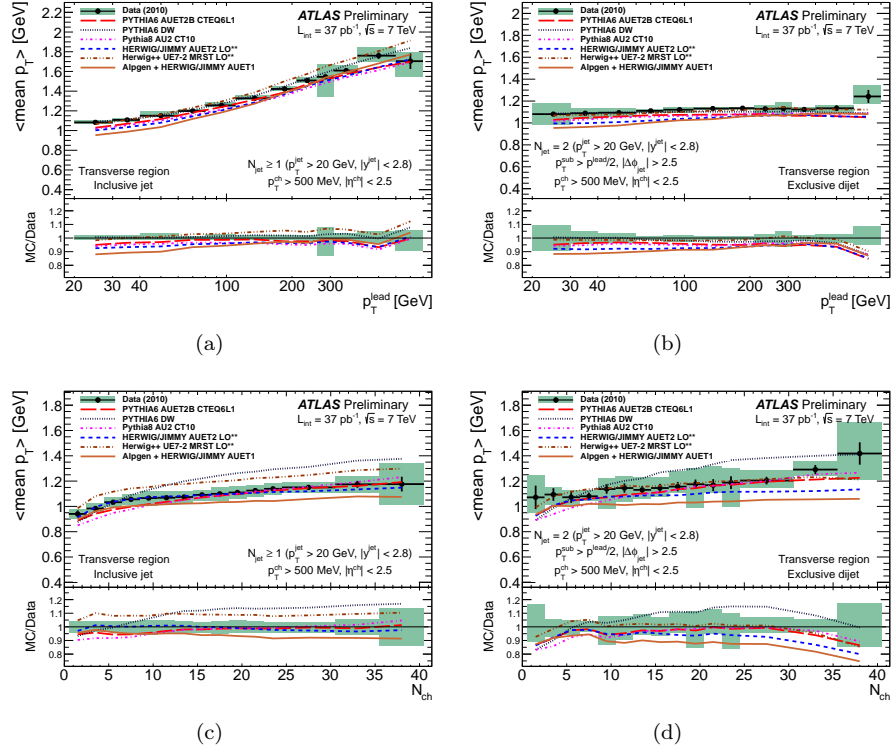


Figure 4: Profile distributions for the mean transverse momentum of charged particles against p_T^{lead} (top) and against the multiplicity of charged particles (bottom) are presented for the inclusive jet (left) and exclusive dijet topology (right). The results are shown for the full transverse region and compared to several Monte Carlo event generator predictions. The black error bar indicate the statistical uncertainty on the data measurements and the green shaded area the combined statistical and systematic uncertainty. Results are taken from [2].

- [3] M. Cacciari, G. Salam, and G. Soyez *Journal of High Energy Physics* **04** (2008) 063.
- [4] W. Lampl, S. Laplace, D. Lelas, et al. No. ATL-LARG-PUB-2008-002. Apr, 2008. <https://cdsweb.cern.ch/record/1099735>.
- [5] ATLAS Collaboration *New J.Phys.* **13** (2011) 053033, [arXiv:1012.5104](https://arxiv.org/abs/1012.5104) [[hep-ex](#)].
- [6] ATLAS Collaboration *JHEP* **1211** (2012) 033, [arXiv:1208.6256](https://arxiv.org/abs/1208.6256) [[hep-ex](#)].
- [7] G. D'Agostini *Nucl. Instrum. Meth.* **A362** (1995) 487–498.
- [8] T. Sjostrand, S. Mrenna, and P. Skands *JHEP* **05** (2006) 026, [hep-ph/0603175](https://arxiv.org/abs/hep-ph/0603175).
- [9] ATLAS Collaboration Oct, 2010. <http://cdsweb.cern.ch/record/1303025>. ATL-PHYS-PUB-2010-014.
- [10] CDF Collaboration, R. Field 2006. FERMILAB-PUB-06-408-E.
- [11] T. Sjostrand, S. Mrenna, and P. Skands *Comput. Phys. Commun.* **178** (2008) 852–867, [arXiv:0710.3820](https://arxiv.org/abs/0710.3820) [[hep-ph](#)].
- [12] ATLAS Collaboration Jul, 2011. <http://cdsweb.cern.ch/record/1363300>. ATL-PHYS-PUB-2011-009.
- [13] M. Guzzi, P. Nadolsky, E. Berger, H.-L. Lai, F. Olness, et al. [arXiv:1101.0561](https://arxiv.org/abs/1101.0561) [[hep-ph](#)].
- [14] G. Corcella et al. [arXiv:hep-ph/0210213](https://arxiv.org/abs/hep-ph/0210213).
- [15] M. L. Mangano, M. Moretti, F. Piccinini, R. Pittau, and A. D. Polosa *JHEP* **0307** (2003) 001, [arXiv:hep-ph/0206293](https://arxiv.org/abs/hep-ph/0206293) [[hep-ph](#)].
- [16] J. Pumplin, D. Stump, J. Huston, H. Lai, P. M. Nadolsky, et al. *JHEP* **0207** (2002) 012, [arXiv:hep-ph/0201195](https://arxiv.org/abs/hep-ph/0201195) [[hep-ph](#)].
- [17] S. Gieseke, C. Rohr, and A. Siodmok [arXiv:1110.2675](https://arxiv.org/abs/1110.2675) [[hep-ph](#)].